Inorg. Chem. **2003**, *42*, 1857−1867

Dioxo-Bridged Dinuclear Manganese(III) and -(IV) Complexes of Pyridyl Donor Tripod Ligands: Combined Effects of Steric Substitution and Chelate Ring Size Variations on Structural, Spectroscopic, and Electrochemical Properties

Yilma Gultneh,* Teshome B. Yisgedu, Yohannes T. Tesema, and Ray J. Butcher

Department of Chemistry, Howard University, Washington, D.C. 20059

Received February 15, 2002

The syntheses and structural, spectral, and electrochemical characterization of the dioxo-bridged dinuclear Mn(III) complexes $[LMn(\mu\text{-}O)_2MnL](ClO_4)_2$, of the tripodal ligands tris(6-methyl-2-pyridylmethyl)amine (**L**[1]) and bis(6-methyl-2-pyridylmethyl)(2-(2-pyridyl)ethyl)amine (**L**[2]), and the Mn(II) complex of bis(2-(2-pyridyl)ethyl)(6-methyl-2-pyridylmethyl)-amine (**L**[3]) are described. Addition of aqueous H_2O_2 to methanol solutions of the Mn(II) complexes of **L**[1] and **L**[2] produced green solutions in a fast reaction from which subsequently precipitated brown solids of the dioxo-bridged dinuclear complexes **1** and **2**, respectively, which have the general formula $[LMn^{III}(\mu\text{-}O)_2Mn^{III}L](ClO_4)_2$. Addition of 30% aqueous H_2O_2 to the methanol solution of the Mn(II) complex of **L**[3] ($[Mn^{II}L^3(CH_3CN)(H_2O)](ClO_4)_2$ (**3**)) showed a very sluggish change gradually precipitating an insoluble black gummy solid, but no dioxo-bridged manganese complex is produced. By contrast, the Mn(II) complex of the ligand bis(2-(2-pyridyl)ethyl)(2-pyridylmethyl)amine (**L**[3a]) has been reported to react with aqueous H_2O_2 to form the dioxo-bridged $Mn^{III}Mn^{IV}$ complex. In cyclic voltammetric experiments in acetonitrile solution, complex **1** shows two reversible peaks at $E_{1/2} = 0.87$ and 1.70 V (vs Ag/AgCl) assigned to the $Mn^{III}{}_2 \leftrightarrow Mn^{III}Mn^{IV}$ and the $Mn^{III}Mn^{IV} \leftrightarrow Mn^{IV}{}_2$ processes, respectively. Complex **2** also shows two reversible peaks, one at $E_{1/2} = 0.78$ V and a second peak at $E_{1/2} = 1.58$ V (vs Ag/AgCl) assigned to the $Mn^{III}{}_2 \leftrightarrow Mn^{III}Mn^{IV}$ and $Mn^{III}Mn^{IV} \leftrightarrow Mn^{IV}{}_2$ redox processes, respectively. These potentials are the highest so far observed for the dioxo-bridged dinuclear manganese complexes of the type of tripodal ligands used here. The bulk electrolytic oxidation of complexes **1** and **2**, at a controlled anodic potential of 1.98 V (vs Ag/AgCl), produced the green $Mn^{IV}{}_2$ complexes that have been spectrally characterized. The Mn(II) complex of **L**[3] shows a quasi reversible peak at an anodic potential of $E_{p,a}$ of 1.96 V (vs Ag/AgCl) assigned to the oxidation Mn(II) to Mn(III) complex. It is about 0.17 V higher than the $E_{p,a}$ of the Mn(II) complex of **L**[3a]. The higher oxidation potential is attributable to the steric effect of the methyl substituent at the 6-positon of the pyridyl donor of **L**[3].

Introduction

There is considerable interest in studies of the high oxidation state complexes of manganese because of their potential uses as oxidizing agents, catalysts,[1] and electrocatalysts[2] for the oxidation of compounds such as alcohols, ethers, and water.[3,4] The involvement of dioxo-bridged dinuclear complexes of high-valent Mn, Fe, Cu, and Ni in aliphatic and aromatic C−H activation and oxygen insertion (monooxygenase) reactions have been reported.[5] The S_2 state of the photosynthetic water oxidizing complex in photosystem II (PS II) shows EPR and X-ray absorption evidence of a dinuclear center with a Mn−Mn distance of about 2.7 Å in common with structurally well characterized synthetic dioxo-bridged dinuclear Mn(III)/Mn(IV) complexes.[6] Thus,

* To whom correspondence should be addressed. E-mail: ygultneh@howard.edu.

(1) (a) Srinivasan, K.; Michand, P.; Kochi, J. K. *J. Am. Chem. Soc.* **1986**, *108*, 2309. (b) Ray, M.; Mukerjee, S.; Mukerjee, R. N. *J. Chem. Soc., Dalton. Trans.* **1990**, 3635. (c) Sharma, Y. R.; Prakash, P. K. S. *Indian J. Chem.* **1980**, *19A*, 1175−1178.

(2) (a) Goodson, P. A.; Oki, A. R.; Glerup, J.; Hodgson, D. J. *J. Am. Chem. Soc.* **1990**, *112*, 6248−6254. (b) Plaskin, P. M.; Stoufer, R. C.; Mathew, M.; Palenick, G. J. *J. Am. Chem. Soc.* **1972**, *94*, 2121−2122.

(3) Gref, A.; Balavoine, G.; Riviere, H.; Andrieux, C. P. *Nuov. J. Chim.* **1984**, *8*, 615−618.

(4) Ramrai, R.; Kira, A.; Kaneko, M. *Angew. Chim., Int. Ed. Engl.* **1986**, *25*, 825−827.

10.1021/ic020131w CCC: $25.00
Published on Web 02/14/2003

Scheme 1. Stable Isolated Dioxo-Bridged Complexes Obtained by the Oxidation, in Solution, of Mn(II) Complexes of Tripodal Pyridyl Donor Amines by Aqueous H_2O_2 (See Figure 1 for Structures of Ligands)[a]

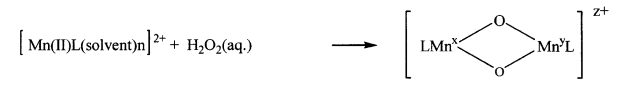

1. x = y = III

   L = L^{1} ‡ **(1)**,Φ L^{1a} ¥ **(1a)**, L^{2} ‡ **(2)**

2. x = III, y = IV

   L = L^{1c} £ **(1c)**, L^{2a} § **(2a)** ; L^{2b} §, † **(2b)** ; L^{3a} ¶ **(3a)**

3. x = y = IV

   L = L^{2a} §

[a] Key: (‡) this work; (Φ) bold numbers (shown here in parentheses) represent the complexes formed by the ligand; (¥) Goodson, P. A.; Oki, A. R.; Glerup, J.; Hodgson, D. J. *J. Am. Chem. Soc.* **1990**, *112*, 6248; (£) Towle, D. K.; Botsford, C. A.; Hodgson, D. J. *Inorg. Chim. Acta* **1988**, *141*, 167; (§) Oki, A. R.; Glerup, J.; Hodgson, D. J. *Inorg. Chem.* **1990**, *29*, 2435; (†) $Mn^{III}Mn^{IV}$ and $Mn^{IV}{}_2$ complexes both isolated but only the structure of the $Mn^{IV}{}_2$ complex reported; (¶) Schindler, S.; Walter, O.; Pederson, J. Z.; Toflund, H. *Inorg. Chim. Acta* **2000**, *303*, 215.

polynuclear manganese complexes have been studied as models for the active sites of these natural systems.[7] Dioxo-bridged $Mn^{III}Mn^{IV}$ complexes of bipyridine[8] and phenanthroline[4] have been reported with the later showing the property of heterogeneously catalyzing the oxidation of water.

A few dioxo-bridged dinuclear $Mn^{III}{}_2$, $Mn^{III}Mn^{IV}$, and $Mn^{IV}{}_2$[9,10] complexes are known (summarized in Scheme 1) that use the tetradentate tripodal tris(2-pyridylalky)amine ligands with the general formula (2-(2-pyridyl)ethyl)$_n$(6-R-2-pyridylmethyl)$_{3-n}$amine (n = 1 or 2, R = H or CH_3) (Figure 1) as well as *N*,*N*′-bis(2-pyridylmethyl)-1,2-ethanediamine, some with methyl substitutions at the 6-position of the pyridyl donors. These have been characterized structurally, spectroscopically, and electrochemically and their catalytic and electrocatalytic properties investigated.[11] Methyl substitution on the pyridyl ring has been found to raise the potential for the Mn(III,III) ↔ $Mn^{III}Mn^{IV}$ and the $Mn^{III}Mn^{IV}$ ↔ Mn(IV,IV) redox processes and consequently stabilize the Mn(III,III) state. This has made possible the preparation and study of dinuclear manganese complexes with a range of oxidation states.[12] Through such steric and steric/ electronic modifications of ligands, a promising pathway has been provided for catalysis or electro-catalysis of the oxidation (or oxygenation) of various target substrates. Higher oxidation potential complexes have greater oxidative capacity for the catalytic or electro-catalytic oxidation of substrates that cannot otherwise be oxidized by complexes of lesser oxidation potentials.

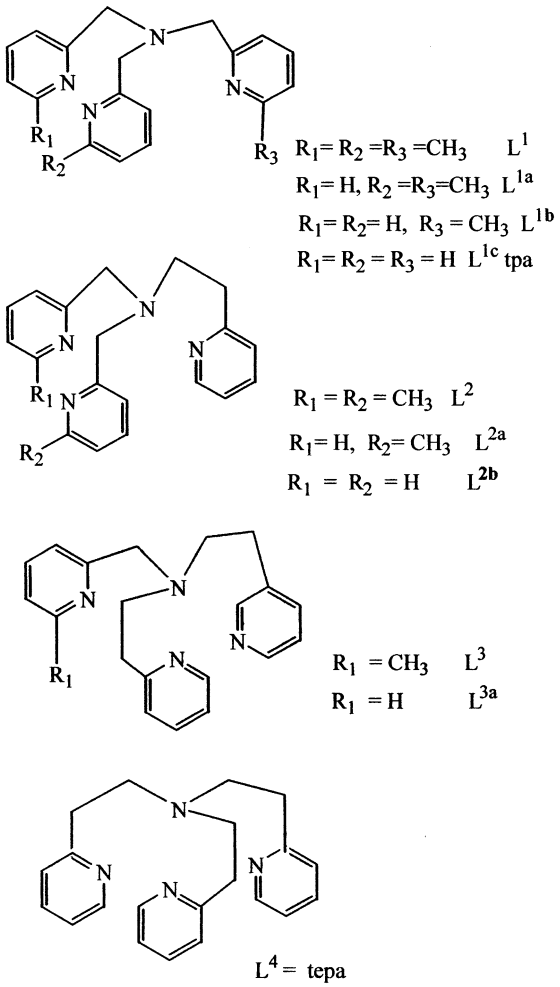

Figure 1. Tripodal pyridyl donor amines.

Here we report the synthesis, structural, electrochemical and spectral characterization of two dioxo-bridged dinuclear manganese(III) complexes, **1** and **2** respectively, of the related tripodal ligands tris(6-methyl-2-pyridylmethyl)amine (**L**[1]), bis(6-methyl-2-pyridylmethyl)(2-(2-pyridyl)ethyl)amine

(5) (a) Itoh, S.; Bandoh, H.; Nagatomo, S.; Kitagawa, T.; Fukuzumi, S. *J. Am. Chem. Soc.* **1999**, *121*, 8945−8946. (b) Karlin, K. D.; Hayes, J. C.; Gultneh, Y.; Cruse, R. W.; McKown, J. W.; Hutchinson, J. P.; Zubieta, J. *J. Am. Chem. Soc.* **1984**, *106*, 2121−2121. (c) Halfen, J. A.; Mahapatra, S.; Wilkinson, E. C.; Kaderli, S.; Young, V. C., Jr.; Que, L., Jr.; Zuberbuhler, A. D.; Tolman, W. B. *Science* **1996**, *271*, 1397−1400. (d) Kim, C.; Dong, Y.; Que, L., Jr. *J. Am. Chem. Soc.* **1997**, *119*, 3635−3636. (e). Ito, S.; Nakao, H.; Berreau, L. M.; Kondo, T.; Komatsu, M.; Fukuzumi, S. *J. Am. Chem. Soc.* **1998**, *120*, 2890−2899. (f) Mahadavan, V.; Hou, Z.; Cole, A. P.; Root, D. E.; Lal, T. K.; Solomon, E. I..; Stack, T. D. P. *J. Am. Chem. Soc.* **1997**, *119*, 11996−11997. (g) Kryalov, S. V.; Rybak-Akimova, E. V. *J. Chem. Soc., Dalton Trans*. **1999**, 3335−3336. (h). Blain, I.; Giorgi, M.; De Riggi, I.; Réglier, M. *Eur. J. Ionrg. Chem*. **2000**, 393−398. (i) Chen, D.; Martell, A. E. *J. Am. Chem. Soc.* **1990**, *112*, 9411−9412.

(6) (a) Goodson, P. A.; Hodgson, D. J.; Glerup, J.; Michelsen, K.; Weihe, H. *Inorg. Chim. Acta* **1992**, *197*, 141−147. (b). Collins, M. A.; Hodgson, D. J.; Michelsen, K.; Towle, D. K. *J. Chem. Soc., Chem. Commun*. **1987**, 1659−1660.

(7) Wemple, M. W.; Tsai, H.-L.; Wang, S.; Claude, J. P.; Streib, W. E.; Huffman, J. C.; Hendrickson, D. N.; Christou, G. *Inorg. Chem*. **1996**, *35*, 6437.

(8) Nyholm, R. S.; Turco, A. *Chem. Ind.* **1960**, 74−75.

(9) (a) Goodson, P. A.; Hodgson, D. J. *Inorg. Chem*. **1989**, *28*, 3606−3608. (b) Glerup, J.; Goodson, P. A.; Hazell, A.; Hazell, R.; Hodgson, D. J.; Mckenzie, C. J.; Michelsen, K.; Rychlewska, U.; Toflund, H. *Inorg. Chem*. **1994**, *33*, 4105.

(10) Goodson, P. A.; Oki, A. R.; Glerup, J.; Hodgson, J. J. *J. Am. Chem. Soc*. **1990**, *112*, 6248.

(11) (a) Goodson, P. A.; Oki, A. R.; Glerup, J.; Hodgson, D. J. *J. Am. Chem. Soc*. **1990**, *112*, 6248. (b) Goodson, P. A.; Glerup, J.; Hodgson, D. J. *Inorg. Chem*. **1990**, *29*, 503. (c) Towle, D. K.; Botsford, C. A.; Hodgson, D. J. *Inorg. Chim Acta* **1988**, *141*, 167−168. (d) Brewer, J. K.; Liegeois, A.; Otvos, H. W.; Calvin, M.; Spreer, L. O. *J. Chem. Soc., Chem. Commun.* **1988**, 1219−1220.

(12) Glerup, J.; Goodson, P. A.; Hazell, A.; Hazell, R.; Hodgson, D. J.; Mckenzie, C. J.; Michelsen, K.; Rychlewska, U.; Toflund, H. *Inorg. Chem*. **1994**, *33*, 4105−4111.

($\mathbf{L^2}$) respectively, and a Mn(II) complex, **3**, of (6-methyl-2-pyridylmethyl)bis(2-(2-pyridyl)ethyl)amine ($\mathbf{L^3}$) (Figure 1). The three ligands have different chelate arm lengths and pyridyl ring substitutions. The precursor Mn(II) complexes of the first two of these ligands yield stable Mn(III) complexes by reaction with aqueous H_2O_2. In their cyclic voltammetry, these complexes exhibit the highest redox potentials so far reported in this class of complexes for the $Mn^{III}{}_2 \leftrightarrow Mn^{III}Mn^{IV}$ and $Mn^{III}Mn^{IV} \leftrightarrow Mn^{IV}{}_2$ redox processes. The ligand $\mathbf{L^3}$ forms a Mn(II) complex which fails to form dioxo-bridged complex on reaction with aqueous H_2O_2. This has been attributed to a combination of chelate arm length and steric effects of the methyl substituent ortho to the N of the donor pyridyl donor group.

Experimental Section

Warning! *Complexes containing organic compounds and perchlorate anion are liable to be explosive and should be handled with care and in small amounts*.

Materials and Methods. All chemicals and solvents used were reagent grade from Aldrich Chemical Co. The reagents 2-(aminomethyl)pyridine, 2,6-lutidine, *N*-bromosuccinimide, benzoyl peroxide, $NaBH_4$, potassium phthalimide, $Mn(ClO_4)_2 \cdot 6H_2O$, H_2O_2 (30% aqueous solution), $CDCl_3$, NH_4Cl, and NH_3(aq) were used as received. Vinylpyridine was vacuum-distilled just before use. Bis(2-(2-pyridyl)ethyl)amine[13] and bis(2-pyridylmethyl)amine[14] were prepared by literature methods. Solvents were dried and distilled under nitrogen: ether and THF from Na/benzophenone, acetonitrile from CaH_2 (further passed through an activated alumina column), and methanol from $Mg(OCH_3)_2$. Elemental analyses were performed by Desert Analytics (Tucson, AZ) and MHW Laboratories (Phoenix, AZ). Conductance of acetonitrile solutions of the complexes were performed on 1.0 mM solutions using YSI 1.0 mm cell and Fisher Model 50 pH/conductance potentiometer.

Magnetic Susceptibility Measurements. Room-temperature magnetic susceptibility measurements were done using the Johnson-Matthey susceptibility balance with $HgCo(NCS)_4$ as calibration standard and magnetic moments calculated with diamagnetic corrections due to the organic ligand.

Spectroscopic Studies. UV−visible absorption measurements of the complexes were done in acetonitrile solutions in 1 cm quartz cuvettes using a HP-8453A diode array spectrometer. Infrared absorption spectra were taken of samples in mineral oil applied on NaCl plates using a Nicolet Magno 560 FT-IR spectrometer. ^1H and ^{13}C NMR spectra were taken on a GE 300 MHz spectrometer with TMS internal reference.

Cyclic Voltammetry. Cyclic voltammetric, bulk electrolysis, and coulometric experiments were performed using a BAS 100B electrochemical work station with a BAS glassy carbon working microelectrode and Ag/AgCl reference and Pt counter electrodes. Typically, 0.1 M *n*-Bu_4 $NClO_4$ supporting electrolyte and 2.0 mM complex solution in acetonitrile solvent were used.

Bulk Controlled-Potential Electrolytic Oxidation of Complexes 1 and 2. Bulk electrolysis was performed on 0.5 mM solutions of complexes **1** and **2** in acetonitrile with 0.1 M *n*-Bu_4-$NClO_4$ as supporting electrolyte using a BAS 100B electrochemical work station potentiostat. The conditions used are as follows: 15.0 mL of the complex solution was stirred in the electrolysis cell with a magnetic stirrer and a platinum mesh (basket) anodic working electrode and a Ag/AgCl reference electrode dipped in this solution. In a compartment separated by a glass frit, a platinum counter electrode was dipped in 10.0 mL of the 0.1 M *n*-Bu_4NClO_4 supporting electrolyte solution. The applied potential was kept constant at 1.98 V (vs Ag/AgCl electrode).

X-ray Crystallography. Single-crystal structure determinations by X-ray diffraction methods were performed using a Siemens P4S four-circle X-ray diffractometer with a graphite monochromator on the incident beam. A molybdenum anode was used as a source of radiation of wavelength 0.7107 Å. Preliminary crystal parameters and reflections were obtained at room temperature and processed by standard methods.[15] The space group was determined from a statistical examination of the intensities. All the structures are solved by direct methods[16] as implemented in the SHELXTLPC system.[17] The non-hydrogen atoms were refined anistropically and hydrogen atoms isotropically.

Syntheses of Ligands. 6-Methyl-2-(bromomethyl)pyridine (α-Bromo-2,6-lutidine). A 10.0 g (93.3 mmol) amount of 2,6-lutidine was dissolved in 150 mL of carbon tetrachloride, and to the solution was added 16.6 g (93.3 mmol) of NBS and 0.25 g of benzoyl peroxide. The mixture was refluxed for 2.5 h, and an additional portion of 0.1 g of benzoyl peroxide was added. After being refluxed for another 1 h, the solution was cooled overnight. The succinimide precipitate was filtered off, and the filtrate was rotary evaporated under reduced pressure to give a light brown oil. This was distilled under vacuum (bp 75°C at 0.5 mmHg) to give 7.2 g (40%) of a pale pink oil which solidified upon standing in the refrigerator. ^{1}HNMR ($CDCl_3$; δ (ppm)): 7.44 (t, 1 H), 7.11 (d, 1 H), 7.02 (d, 1H), 4.40 (s, 2 H), 2.42 (s, 3 H). C-13 NMR ($CDCl_3$; δ (ppm)): 157.93, 155.64, 136.84, 122.24, 120.08, 33.82, 24.00. GC/MS: *m*/*e* 187/185 (M^+).

6-Methyl-2-pyridylmethylamine. To 5.5 g (29.7 mmol) of α-bromo-2,6-lutidine dissolved in 50 mL of dry DMF was added potassium phthalimide (11.8 g, 63.9 mmol) and sodium bicarbonate (6.38 g, 73.7 mmol). The mixture was refluxed for 3.5 h and cooled to room temperature. The white solid that formed was removed by suction filtration, and the solvent from the filtrate was removed by rotary evaporation. Addition of water (50 mL) to the residue followed by filtration and drying gave 5.3 g (71.5% yield) of the phthalimide derivative product as a white solid. The dried phthalimide derivative was dissolved in glacial acetic acid and refluxed for 48 h, during which time 12 M HCl portions (3 × 6 mL) were added. The solution was filtered and washed with concentrated aqueous HCl, and the filtrate was stripped to dryness under vacuum. Addition of 10 mL of methanol precipitated the hydrochloride salt as white solid. This was dissolved in 15 mL of water made basic (pH > 10) by adding 2 M sodium hydroxide and the free amine extracted with methylene chloride (3 × 40 mL). The extracts were combined, dried over anhydrous magnesium sulfate, and filtered, and the solvent was evaporated at reduced pressure to give 2.2 g (61.3% yield) of the ligand as a colorless oil. ^{1}H NMR ($CDCl_3$−TMS; δ (ppm)): 7.76 (t, 4-H, 1H), 7.31 (d, 5-H, 1 H), 7.23 (d, 3-H, 1 H), 4.16 (s, CH_2, 2 H), 2.78 (s, CH_3, 3 H), 1.94 (s(b), NH_2,

(13) (a) Nelson, S. M.; Rogers, J. *Inorg. Chem*. **1967**, *6*, 1390−1395. (b) Romary, J. K.; Zachariasen, R. D.; Garger, J. D.; Schiesser, H. *J. Chem. Soc. C* **1968**, 2884−2887.
(14) Romary, J. K.; Bund J. E.; Barger, J. D. *J. Chem. Eng. Data* **1967**, *12*, 9.
(15) (a) Storm, C. B.; Freeman, C. M.; Butcher, R. J.; Turner, A. H.; Rowan, N. S.; Johnson, F. O.; Sinn, E. *Inorg. Chem*. **1983**, *22*, 849. (b) Spencer, J. T.; Pourian, M. R.; Butcher, R. J.; Sinn, E.; Grimes, R. N. *Organometallics* **1987**, *2*, 335.
(16) Karle, I. L.; Karle, J. *Acta Crystallogr*. **1966**, *21*, 849.
(17) Sheldrick, G. M. *SHELXTLPC, microcomputer programs for structure determination on a PC*; University of Göttingen: , Germany, 1989.

2 H). C-13 NMR ($CDCl_3$; δ (ppm)): 161.16, 157.54, 136.29, 120.79, 117.594, 47.61, 24.04.

Tris(6-methyl-2-pyridylmethyl)amine (L^1). A 1.03 g (8.44 mmol) of 6-methyl-2-pyridylmethylamine was dissolved in 15.0 mL of distilled water and the solution cooled to 0 °C. To this cooled solution was added 3.14 g (16.9 mmol) of α- bromo-2,6-lutidine which was dissolved in 20.0 mL of dichloromethane. The biphasic mixture was stirred for 1 h, and 0.68 g (16.9 mmol) of NaOH was added. The mixture was left to stir for 3 days, extracted with CH_2Cl_2 (3 × 40 mL), dried with anhydrous $MgSO_4$, and filtered, and the filtrate was rotary-evaporated to give 2.3 g (82.0% yield) of the faint yellow oil product. ^{1}H NMR spectrum ($CDCl_3$; δ (ppm)) (TMS = 0 ppm): 7.50 (t, 4-H, 3H), 7.41 (d, 5-H, 3H), 6.94 (d, 3-H, 3H), 5.25 (s, CH_2Cl_2), 3.83 (s, CH_2, 6H), 2.48 (s, CH_3, 9H). ^{13}C NMR spectrum ($CDCl_3$; δ (ppm)): 159.22, 157.57, 136.42, 121.18, 119.53, 60.40, 24.36.

2-(2-Pyridyl)ethylbis(6-methyl-2-pyridylmethyl))amine (L^2). A 1.2 g (9.83 mmol) amount of 2-(2-pyridyl)ethyl)amine in 10 mL of water at 0 °C was added to 3.66 g (19.67 mmol) of α-bromo-2,6-lutidine dissolved in 10 mL of dichloromethane at 0 °C. This was stirred at 0 °C for 1 h, and 0.79 g of NaOH dissolved in 15 mL of water was added to the mixture. The mixture was stirred for another 2 h at 0 °C, left to stir at room temperature for 72 h, and extracted with dichloromethane (3 × 40 mL), and the extract was washed with distilled water, dried over anhydrous $MgSO_4$, and filtered. The filtrate was evaporated at reduced pressure to give 3.4 g (nearly quantitative amount) of the ligand as a light yellow oil. ^{1}H NMR ($CDCl_3$; δ (ppm)): 8.48 (d, 1H), 7.65 (d, 1H), 7.55 (t, 1H), 7.46 (t, 2H), 7.32 (d, 2H), 7.14 (d, 2H), 5.27 (s, CH_2Cl_2), 3.89 (s, 4 H), 3.04 (m, 4H), 2.54 (s, 6H). ^{13}C-NMR ($CDCl_3$; δ (ppm)): 160.54, 159.22, 157.25, 148.98, 136.42, 135.90, 123.31, 121.15, 120.89, 119.354, 60.334, 54.33, 35.96, 24.33.

Bis-2-(2-pyridyl)ethyl)(6-methyl-2-pyridylmethyl)amine (L^3). This ligand was made by the reaction of bis-2-(2-pyridylethyl)-amine (bpea)[18] and α-bromo-2,6-lutidine. To 2.3 g (10.13 mmol) of bpea in 10 mL of water at 0 °C was added 1.88 g (10.13 mmol) of α-bromo-2,6-lutidine dissolved in 10 mL of dichloromethane also at 0 °C. After the solution was stirring for 1 h, 0.4 g of NaOH in 10 mL of water was added. Stirring was continued for another 2 h at 0 °C and for 72 h more at room temperature. The reaction mixture was extracted with dichloromethane (3 × 40 mL), and the combined extracts were washed with distilled water and dried over anhydrous $MgSO_4$. The filtrate was rotary-evaporated to give 3.4 g (73.4% yield) of the ligand as a light yellow oil. ^{1}H NMR ($CDCl_3$; δ (ppm)): 8.64 (s, 2H), 7.68 (t, 1H), 7.53 (t, 2H), 7.20 (m, 4H), 7.07 (t, 2H), 4.01(s, 2H)), 3.13 (m, 8H), 2.66 (s, 3H). ^{13}C: NMR ($CDCl_3$; δ (ppm)): 160.38, 159.35, 156.86, 148.79, 136.09, 135.65, 123.05, 120.79, 120.629, 119.08, 60.21, 53.94, 35.79, 24.10.

Syntheses of Complexes. $Mn^{III}_2(\mu\text{-oxo})_2(L^1)_2(ClO_4)_2$ (L^1 = Tris(6-methyl-2-pyridylmethyl)amine)) (1). A 1.3 g (3.92 mmol) amount of tris(6-methyl-2-pyridylmethyl)amine (**L^1**) dissolved in 10.0 mL of methanol was added to a methanol solution (10 mL) of 1.42 g (3.92 mmol) of $Mn(ClO_4)_2\cdot 6H_2O$ while stirring. After the mixture was stirred for 1 h, 50.0 mL diethyl ether was added gradually resulting in the separation of a yellow oil. The yellow oil was dissolved in 15.0 mL of methanol, and 2.0 mL of 30% aqueous H_2O_2 solution was added dropwise. The solution turned dark-green, and a brown solid precipitated immediately. Filtration and washing with methanol and diethyl ether gave 0.89 g (45.0%) of brown powdery product. An acetonitrile solution of this solid, layered with ether, gave brown crystals of a quality good for X-ray diffraction structure determination. Anal. Calcd for $C_{42}H_{48}Cl_2Mn_2N_8O_{10}$: C, 50.12; H, 4.81; N, 11.14. Found: C, 50.01; H, 4.96; N, 10.94. IR absorption spectrum (Nujol; cm^{-1}): 3160, 3001, 1645, 1600, 1461, 1366, 1093, 1033, 919, 790, 745, 685, 626.

$Mn^{III}_2(\mu\text{-oxo})_2(L^2)_2(ClO_4)_2$ (2).[19] A 1.88 g (5.65 mmol) amount of the ligand **L^2** was dissolved in 20 mL of methanol and added to 2.05 g (5.65 mmol) of $Mn(ClO_4)_2\cdot 6H_2O$ in 10 mL of methanol. After the solution was stirred for 30 min, 60 mL of diethyl ether was added, which produced a yellow oil. The yellow oil was dissolved in 20 mL of methanol, and on addition of 1.0 mL of 30% aqueous H_2O_2, a green solution resulted. A brown solid precipitated, and the solution changed to colorless. The brown precipitate was filtered out and washed with methanol and diethyl ether to give 1.50 g (53% yield) of the complex. Slow addition of ether to an acetonitrile solution of the complex and standing for several days gave crystals suitable for X-ray diffraction structure determination. Anal. Calcd for $C_{42}H_{48}Cl_2Mn_2N_8O_{10}$: C, 50.20; H, 4.86; N, 11.14. Found: C, 50.38; H, 5.30; N, 10.78. IR (Nujol; cm^{-1}): 1610, 1565, 1461, 1381, 1297, 1172, 1073, 973, 825, 795, 725, 676, 615.

$[MnL^3(CH_3CN)(H_2O)](ClO_4)_2$ (3). A solution of 3.2 g (10.0 mmol) of the ligand **L^3** in 10 mL of methanol was added to 3.65 g (10.0 mmol) of $Mn(ClO_4)_2\cdot 6H_2O$ while stirring. After the dark brown solution was stirred for 30 min, addition of 100 mL of ether precipitated a colorless solid which was filtered out, washed with 10 mL of methanol/ether mixture, and dried under vacuum, yielding the nearly quantitative amount of 5.2 g (yield 80.1%) of a colorless powder. Diamond-shaped crystals, suitable for X-ray crystallographic structure determination, were obtained by layering an acetonitrile solution of the complex with ether and standing for several days. Anal. Calcd for $C_{23}H_{29}Cl_2MnN_5O_9$: C, 42.77; H, 4.50; N, 10.85. Found: C, 43.09; H, 4.80; N, 10.85.

Results and Discussion

Reactions of Mn(II) Complexes of L^1 and L^2 with Aqueous H_2O_2. The reactions of **L^1** and **L^2** with $Mn(ClO_4)_2\cdot 6H_2O$ in methanol produce colorless Mn(II) complexes which separate as oil on addition of ether. In each case, on addition of excess amounts of 30% aqueous solution of H_2O_2 to the methanol solution of the Mn(II) complex, first a dark green solution forms quickly which is then followed by precipitation of a brown powdery solid (shown to be complexes **1** and **2)** under a nearly colorless solution. The formation and precipitation of complex **1** was fast after the appearance of the green solution, whereas, the green solution formed stayed for about 5 min before the start of precipitation of the brown powdery form of complex **2**. Figure 2 shows the UV−visible absorption spectra, taken at intervals of time, of the solution of the reaction mixture, during the progress of the reaction of the Mn(II) complex of **L^2** in CH_3CN solution after the addition of 30% aqueous H_2O_2. It shows the appearance and growth with time of a peak at 552 nm corresponding to the formation and buildup in concentration, of the dioxo-bridged

(18) Gultneh, Y.; Khan, A. R.; Blaise, D.; Chaudhry, S.; Ahvazi, B.; Marvery, B. B.; Butcher, R. J. *J. Inorg. Biochem.* **1999**, *75*, 7.

(19) In the crystal structure of complex **2**, two acetonitrile molecules of crystallization are observed/dioxo-bridged unit. However the elemental analysis (shown below) data for the bulk fit the formulation without the acetonitrile molecules indicating that these solvent molecules are lost over time. Therefore, the fomulation by elemental analysis is as shown here. The formulation by the crystallographic structure shows two CH_3CN molecules. See the crystal packing diagram in the Supporting Information.

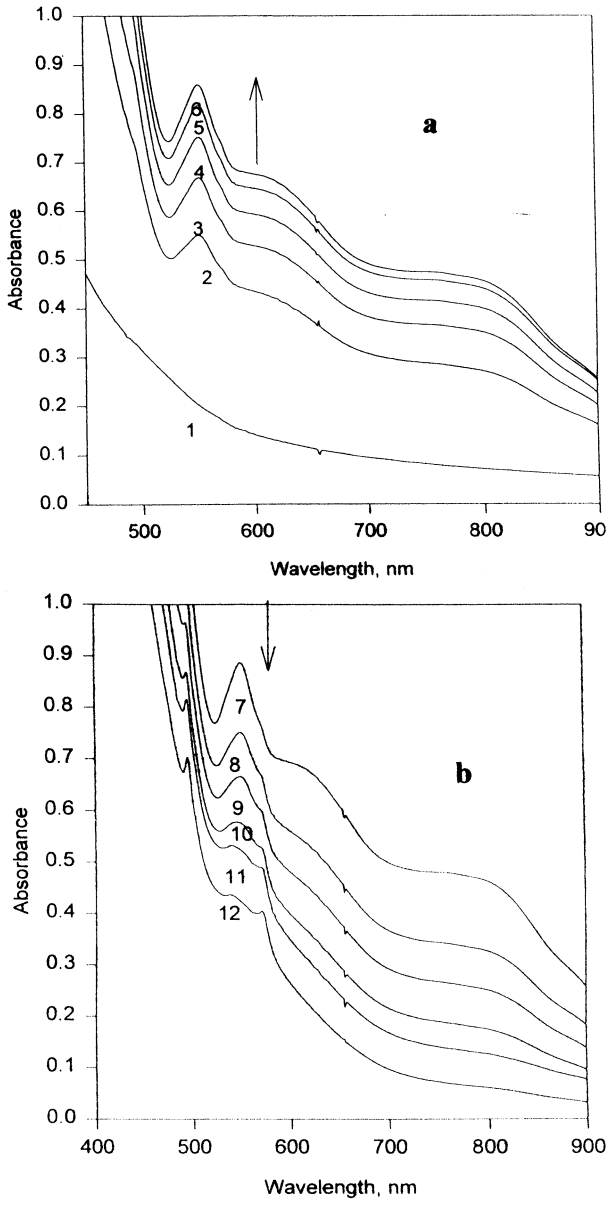

Figure 2. Electronic absorption spectra of the reaction mixture of the Mn(II) complex of $\mathbf{L^2}$ in methanol (2.5×10^{-3} M) with aqueous H_2O_2 taken at intervals of time during the progress of the reaction showing the formation and buildup in concentration of the green Mn^{IV}_2 complex (a) and the subsequent decrease in the concentration of the green complex with conversion to the brown solution of the Mn^{III}_2 complex (b).

dinuclear Mn^{IV}_2 complex (see below) over the first approximately 3 min period followed by the decline of this peak and the appearance and growth of much weaker absorbance peaks (superimposed on the much stronger absorbance of the green solution) at 496 and 571 nm corresponding with the conversion of the green Mn^{IV}_2 complex to the more stable Mn^{III}_2 complex that is isolated as the stable brown complex **2** (see below).

Measurement of the absorbance at 552 nm was used to follow the progress of the reaction of the Mn(II) complex of $\mathbf{L^2}$ with 30% aqueous H_2O_2 in acetonitrile solution, under pseudo-first-order conditions to determine the dependence of the rate on the concentrations of the Mn(II) complex and H_2O_2. Plot of $\log(A_0 - A_t)/(A_t - A_\infty)$ vs t gave a straight line showing the first-order kinetics in each reactant. The second-order rate constant was calculated to be 0.075 M^{-1} s^{-1}. The bulk electrolytic oxidation of the Mn^{III}_2 brown complexes **1** and **2** dissolved in acetonitrile produced green solutions with coulometric measurements that are consistent with 2-electron oxidation of each dinuclear unit (see discussion below). The green solutions thus produced show electronic absorption spectra identical to those of the green solutions first produced from the H_2O_2 reactions with the Mn(II) complexes as described above.

Crystal Structures of Complexes 1−3. Table 1 gives the crystal data and structure refinement. Tables 2−4 show selected bond distances and angles in complexes **1**−**3**. The ORTEP diagrams of the coordination in the cations are shown in Figures 3−5.

Structures of $[L^1Mn(\mu\text{-oxo})_2Mn(L^1)](ClO_4)_2$ (1) and $[L^2Mn(\mu\text{-oxo})_2MnL^2](ClO_4)\cdot 2.2CH_3CN$ (2). Tables 2 and 3 show selected bond angles and distances in the structures of complexes **1** and **2**, respectively. Although these complexes were both synthesized and recrystallized from acetonitrile/ether solvents in identical manner, complex **2** crystallized with two acetonitrile solvent molecules/dinuclear unit as shown by the crystallographic structure, while complex **1** crystallized without any solvent molecules. However, the crystals of complex **2** also lose all solvent molecules on standing as shown by the elemental analysis. The crystal structures of these two complexes are similar with slight differences in coordination bond angles. In both complexes, two Mn(III) ions are bridged by two oxo ligands and each one coordinated by one molecule of the tetradentate tripodal ligand. The geometry about each Mn ion is a distorted octahedron. The Mn−Mn distances (2.7042(5) Å in **1** and 2.712(1) and 2.707(1) Å in **2**[20]) show slight difference. In each case, two N_{py} donors of the 6-methyl-2-pyridylmethyl chelating arms occupy the trans axial positions at each Mn(III) ion with $N_{py}-Mn-N_{py}$ angle of 147.58(6)° in complex **1** and 148.4(1)° in complex **2**. The axial $Mn-N_{py}$ bonds (average length of 2.4013(16) Å in **1** and 2.369(4) Å in **2**) are distinctly longer than the equatorial $Mn-N_{py}$ bonds (2.159(1) Å in **1** and 2.143(3**)** Å in **2**) and the $Mn-N_{amine}$ bond (2.125(1) Å) which are attributable to the expected Jahn−Teller distortion of the coordination of d^4 Mn(III) in an octahedral ligand field. The $Mn-N_{axial}$ bonds are also about 0.20 Å longer than the corresponding bonds (2.206(4) Å and 2.260 Å) in the $Mn^{III}Mn^{IV}$ complex of tpa,[11c] most likely due to the steric effect of methyl substitutions in **1** and **2.** The $N_{amine}-Mn-N_{axial}$ chelate angles are about 74.2° in both **1** and **2**. The $N_{amine-}Mn-N_{equatorial}-$pyridyl chelate angle in **1** (82.26(6)°) is smaller than in **2** (93.4(1)°) due to the longer 2-(2-pyridyl)ethyl chelate arm in **2**. The Mn_2O_2 unit is planar in each structure with the sum of internal angles of 360°. The four equatorial donors around each Mn(III) ion also form an average plane which includes the Mn(III) ion as shown by the sum of the angles made by an axial group with the equatorial donors at Mn which is 360°. The $N_{py(equatorial)-}Mn-O_{oxo}$ cis angle is 104.01(5)°, while the

(20) Complex **2**, in its crystal structure, shows two crystallographically nonequivalent but chemically equivalent dioxo-bridged dinuclear units with slightly different Mn···Mn bond distances.

Table 1. Crystal Data and Structure Refinement for Complexes **1**−**3**

param	**1**	**2**	**3**
emp formula	$C_{42}H_{48}Cl_2Mn_2N_8O_{10}$	$C_{46}H_{54}Cl_2Mn_2N_{10}O_{10}$	$C_{23}H_{29}Cl_2MnN_5O_9$
fw	1005.66	1087.77	645.35
temp (K)	293(2)	293(2)	293(2)
wavelength (Å)	0.710 73	0.710 73	0.710 73
cryst system	triclinic	triclinic	monoclinic
space group	$P\bar{1}$	$P\bar{1}$	Cc
unit cell dimens (Å, deg)	$a = 9.0081(7)$	$a = 12.3508(18)$	$a = 21.053(2)$
	$b = 11.5256(10)$	$b = 14.950(2)$	$b = 10.9427(9)$
	$c = 11.8101(10)$	$c = 15.1856(16)$	$c = 15.5772(16)$
	$\alpha = 65.628(6)$	$\alpha = 78.751(9)$	$\beta = 127.582(7)$
	$\beta = 80.426(7)$	$\beta = 68.485(8)$	
	$\gamma = 86.505(7)$	$\gamma = 76.168(10)$	
V (Å^3), Z	1102.26(16), 2	2514.9(6), 2	2843.9(5), 4
density (calcd) (mg/mL)	1.515	1.436	1.507
abs coeff (mm^{-1})	0.761	0.674	0.710
F(000)	520	1128	1332
θ range data collcn (deg)	2.10−27.50	2.04−27.50	2.23−27.50
limiting indices	$-11 \le h \le 0$	$0 \le h \le 15$	$0 \le h \le 24$
	$-13 \le k \le 13$	$-18 \le k \le 19$	$-14 \le k \le 0$
	$-15 \le l \le 15$	$-18 \le l \le 19$	$-20 \le l \le 16$
reflcns collcd	5236	11 938	3291
indepndt reflcns	4928 ($R_{int} = 0.0145$)	11 405 ($R_{int} = 0.0396$)	3291($R_{int} = 0.000$)
completeness to $\theta = 27.50°$ (%)	97.2	98.9	98.0
abs corr	SHELXA	SHELXA	SHELXA
max/min transm	0.8673 and 0.5658	0.7842 and 0.3781	0.9107 and 0.6879
refinement method	full matrix least squares on F^2	full matrix least squares on F^2	full matrix least squares on F^2
data/restraints/params	4928/0/317	11 405/29/717	3291/31/429
goodness of fit on F^2	1.081	1.003	1.026
final R indexes [$I > 2\sigma(I)$]	R1 = 0.0356	R1 = 0.0653	R1 = 0.0397
	wR2 = 0.0976	wR2 = 0.1508	wR2 = 0.0963
R indices (all data)	R1 = 0.0386	R1 = 0.1253	R1 = 0.0579
	R1 = 0.0386	wR2 = 0.1829	wR2 = 0.1093
extinction coeff	0.034(3)		0.0021(4)
largest diff peak and hole (e Å^{-3})	0.283 and −0.226	0.568 and −0.430	0.283 and −0.226

Table 2. Selected Bond Distances (Å) and Angles (deg) in Complex **1**

Bond Distances (Å)			
Mn−O	1.8264(12)	Mn−O$^{\#1}$	1.8285(12)
Mn−N	2.1253(15)	Mn−N(1C)	2.1592(14)
Mn−N(1B)	2.3982(16)	Mn−N(1A)	2.4044(17)
Mn−Mn$^{\#1}$	2.7042(5)		
Bond Angles (deg)			
Mn−O−Mn$^{\#1}$	95.44(6)	O−Mn−O$^{\#1}$	84.56(6)
O−Mn−N	173.69(5)	O$^{\#1}$−Mn−N	89.17(5)
O−Mn−N(1C)	104.01(5)	O$^{\#1}$−Mn−N(1C)	171.43(5)
N−Mn−N(1C)	82.26(6)	O−Mn−N(1B)	105.14(6)
O$^{\#1}$−Mn−N(1B)	93.36(6)	N−Mn−N(1B)	74.57(6)
N(1C)−Mn−N(1B)	84.33(5)	O−Mn−N(1A)	106.85(6)
O$^{\#1}$−Mn−N(1A)	94.73(6)	N−Mn−N(1A)	74.21(6)
N(1C)−Mn−N(1A)	83.03(6)	N(1B)−Mn−N(1A)	147.58(6)
O−Mn−Mn$^{\#1}$	42.31(4)	O$^{\#1}$−Mn−Mn$^{\#1}$	42.25(4)
N−Mn−Mn$^{\#1}$	131.41(4)	N(1C)−Mn−Mn$^{\#1}$	146.32(4)
N(1B)−Mn−Mn$^{\#1}$	102.48(4)	N(1A)−Mn−Mn$^{\#1}$	104.57(4)

$N_{py(axial)}$−Mn−O_{oxo} cis angles are 105.14(6) and 106.85(6)° for one of the two bridging oxo ligands and 93.36(6) and 94.73(6)° for the second oxo ligand in complex **1**. In complex **2**, the $N_{py(equatorial)}$−Mn−O_{oxo} cis angle is 92.9(1)° while the $N_{py(axial)}$−Mn−O_{oxo} cis angles are 107.1(1)° and 104.0(1)° for one of the two bridging oxo ligands and 93.6(1) and 94.0(1)° for the second oxo ligand.

Structural Effects of Methyl Substitutions and Chelate Ring Expansions. Table 5 shows selected bond angles and distances in the dioxo-bridged Mn^{III}_2, $Mn^{III}Mn^{IV}$, and Mn^{IV}_2 complexes of some tripodal pyridyl donor amines (each obtained by the oxidation of the Mn(II) complexes by addition of aqueous H_2O_2) as reported in the literature and from this work. While the complex of tpa (tris(2-pyridylmethy)amine) (**L^{1c}**) is isolated as stable $Mn^{III}Mn^{IV}$,[21] all the isolated stable complexes of the derivatives of tpa with 6-methyl-substitution on the pyridyl donors are Mn^{III}_2 complexes. This shows the greater stability of the lower oxidation state as a result of methyl substitution at the 6-position of the pyridyl rings. The Jahn−Teller lengthening of the Mn−N axial bonds in Mn(III) coordination decreases the unfavorable steric interactions of methyl groups and thus makes the Mn(III) state more stable. This leads to the isolation of the Mn^{III}_2 complexes **1**, **2**, and **1a**[22] as the more stable products. In comparison of the bond distances and angles in the analogous Mn^{III}_2 complexes, **1** vs **1a** (the dioxo-bridged Mn^{III}_2 complex of ligand **L^{1a}**), the effect of one methyl substitution on the equatorially coordinated pyridyl group causes increases in the Mn−Mn (0.03 Å), Mn−O_{oxo} (0.01 Å), the equatorial Mn−N_{py} (0.08 Å), and the axial Mn−N_{py} (0.03 Å) bond distances and decreases the O−Mn−O angle (1.5°), the trans O−Mn−N_{amine} angle (about 6°), and the trans O−Mn−N_{py} angle (about 3.5 °) relative to the analogous complex of the ligand **L^{1a}**.

The steric effect of methyl substitution on the structure is also seen in the differences in the axial N_{py}−Mn−N_{py} angles. These angles are about 10° less in the complexes of the ligands with substituted pyridyl donors (complexes **1**, **1a**, and **2**: average 147.57(6)°) than in the complex with the nonsubstituted pyridyl donors (complex **2b**: 158.0°). This angle is also some 16.4° less in complex **2** (148.4(1)°) than

(21) See Figure 1 for structures and symbols used for ligands.
(22) See Scheme 1 for the designations of complexes.

Table 3. Selected Bond Lengths (Å) and Angles (deg) in Complex **2**

Bond Lengths (Å)			
Mn(1)−Mn(1)$^{\#1}$	2.7067(11)	Mn(2)−Mn(2)$^{\#2}$	2.7119(12)
O(1)−Mn(1)$^{\#1}$	1.830(2)	O(2)−Mn(2)$^{\#2}$	1.829(3)
Mn(1)−N(1)	2.137(3)	Mn(2)−N(2)	2.149(3)
Mn(1)−O(1)	1.822(3)	Mn(2)−O(2)	1.826(3)
Mn(1)−O(1)$^{\#1}$	1.830(2)	Mn(2)−O(2)$^{\#2}$	1.829(3)
Mn(1)−N(1A)	2.143(3)	Mn(2)−N(2A)	2.149(3)
Mn(1)−N(1B)	2.330(4)	Mn(2)−N(2B)	2.398(4)
Mn(1)−N(1C)	2.390(4)	Mn(2)−N(2C)	2.358(4)
Bond Angles (deg)			
Bond Angles about Mn(1)			
O(1)−Mn(1)−O(1)$^{\#1}$	84.33(12)	O(1)−Mn(1)−N(1)	89.44(12)
O(1)$^{\#1}$−Mn(1)−N(1)	173.30(13)	O(1)−Mn(1)−N(1A)	174.73(13)
O(1)$^{\#1}$−Mn(1)−N(1A)	92.97(12)	N(1)−Mn(1)−N(1A)	93.43(13)
O(1)−Mn(1)−N(1B)	93.68(12)	O(1)$^{\#1}$−Mn(1)−N(1B)	107.17(12)
N(1)−Mn(1)−N(1B)	75.63(13)	N(1A)−Mn(1)−N(1B)	82.77(13)
O(1)−Mn(1)−N(1C)	94.09(13)	O(1)$^{\#1}$−Mn(1)−N(1C)	104.02(13)
N(1)−Mn(1)−N(1C)	73.90(13)	N(1A)−Mn(1)−N(1C)	90.96(13)
N(1B)−Mn(1)−N(1C)	148.43(12)	O(1)−Mn(1)−Mn(1)$^{\#1}$	42.28(8)
O(1)$^{\#1}$−Mn(1)−Mn(1)$^{\#1}$	42.05(8)	N(1)−Mn(1)−Mn(1)$^{\#1}$	131.68(10)
N(1A)−Mn(1)−Mn(1)$^{\#1}$	134.85(10)	N(1B)−Mn(1)−Mn(1)$^{\#1}$	104.05(9)
N(1C)−Mn(1)−Mn(B)$^{\#1}$	102.23(9)	Mn(1)−O(1)−Mn(1)$^{\#1}$	95.67(12)
Bond Angles about Mn(2)			
O(2)−Mn(2)−O(2)$^{\#2}$	84.20(12)	Mn(2)−O(2)−Mn(2)$^{\#2}$	95.80(12)
O(2)−Mn(2)−N(2A)	92.95(13)	O(2)$^{\#2}$−Mn(2)−N(2A)	176.32(12)
O(2)−Mn(2)−N(2)	173.88(13)	O(2)$^{\#2}$−Mn(2)−N(2)	89.98(13)
N(2A)−Mn(2)−N(2)	92.94(13)	O(2)−Mn(2)−N(2C)	106.91(12)
O(2)$^{\#2}$−Mn(2)−N(2C)	94.10(12)	N(2A)−Mn(2)−N(2C)	84.49(13)
N(2)−Mn(2)−N(2C)	75.32(13)	O(2)−Mn(2)−N(2B)	104.36(13)
O(2)$^{\#2}$−Mn(2)−N(2B)	93.50(12)	N(2A)−Mn(2)−N(2B)	89.46(13)
N(2)−Mn(2)−N(2B)	74.04(13)	N(2C)−Mn(2)−N(2B)	148.39(13)
O(2)−Mn(2)−Mn(2)$^{\#2}$	42.14(8)	O(2)$^{\#2}$−Mn(2)−Mn(2)$^{\#2}$	42.06(8)
N(2A)−Mn(2)−Mn(2)$^{\#2}$	135.05(10)	N(2)−Mn(2)−Mn(2)$^{\#2}$	132.92(90
N(2C)−Mn(2)−Mn(2)$^{\#2}$	104.13(9)	N(2B)−Mn(2)−Mn(2)$^{\#2}$	102.02(9)

Table 4. Selected Bond Lengths (Å) and Angles (deg) in Complex **3**

Bond Lengths (Å)			
Mn−O(1W)	2.242(5)	Mn−N	2.301(4)
Mn−N(1A)	2.247(5)	M−N(1B)	2.290(4)
Mn−N(1C)	2.283(5)	Mn−N(1S)	2.284(5)
Bond Angles (deg)			
O(1W)−Mn−N(1A)	90.7(2)	O(1W)−Mn−N(1B)	166.05 (19)
O(1W)−Mn−N(1C)	84.9(2)	O(1W)−Mn−N(1S)	78.6(2)
O(1W)−Mn−N	102.0(2)	N(1A)−Mn−N(1B)	92.28(17)
N(1A)−Mn−N(1C)	159.08(17)	N(1A)−Mn−N	85.61(17)
N(1A)−Mn−N(1S)	88.86(19)	N(1B)−Mn−N	91.86(15)
N(1C)−Mn−N(1B)	96.92(15)	N(1C)−Mn−N(1S)	110.16(18)
N(1S)−Mn−N(1B)	87.85(17)	N(1C)−Mn−N	75.38(17)
N(1S)−Mn−N	174.45(19)		

in the complex **3a** (the dioxo-bridged Mn^{III}_2 complex of ligand $\mathbf{L^{3a}}$) (164.4°) (see Table 5). The decrease in the axial trans angles with methyl substitution is attributable to increased steric repulsions across the dioxo bridge.

The differences between the structural parameters of **1a** and **2**, which show the effect of the expansion of one chelate ring, are similar to those shown by the effects of methyl substitutions in complexes **1** and **1a**. The O−Mn−O angle shows a decrease of about 1.9° from the $Mn^{III}Mn^{IV}$ complex of $\mathbf{L^{2b}}$ to that of $\mathbf{L^{3a}}$ while the Mn−Mn distances show increase from 2.643 to 2.693 to 2.739 Å in the $Mn^{III}Mn^{IV}$ series of the complexes of tpa, $\mathbf{L^{2b}}$, and $\mathbf{L^{3a}}$, respectively.

Structure of $[Mn^{II}L^3(CH_3CN)(H_2O)](ClO_4)_2$ (3). The ORTEP drawing of the cation of this complex is shown in Figure 5. The Mn(II) ion is coordinated in a distorted octahedral geometry formed by the four donor groups from the ligand $\mathbf{L^3}$, an acetonitrile, and a H_2O molecule. The

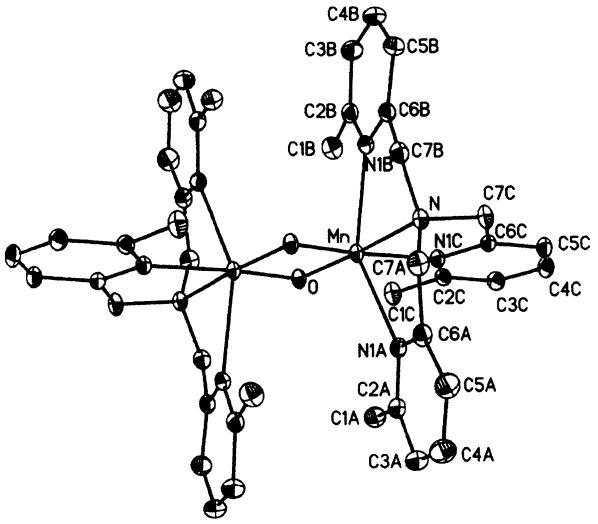

Figure 3. ORTEP drawing of the coordination in the cation of complex **1**.

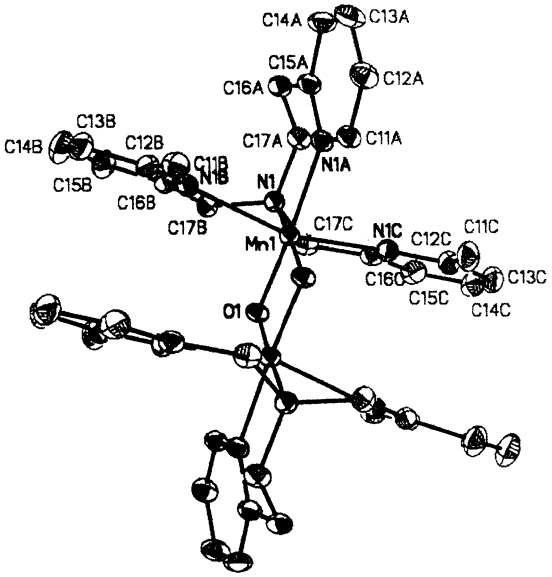

Figure 4. ORTEP drawing of the coordination in the cation of complex **2**.

chelate and the cis coordination angles are close to right angles except for the chelate angle that includes the methyl-substituted 2-pyridylmethyl arm (75.3(1)°), a consequence of the small bite angle. Goodson et al. have found[2b] that the methyl group on the 6-position of the pyridyl donor in the ligand $\mathbf{L^{1a}}$ increased the axial Mn−N bond length in the Mn(II) complex. In complex **3**, the $Mn-N_{py}$ bond length of the methyl-substituted pyridyl (2.283(5) Å) is not significantly different from those of the other Mn−N bonds. However, the present ligand appears to force an N_{CH_3CN}−Mn−O_{OH_2} angle of 78.6(2)°, which is significantly smaller than the O−Mn−O angles (ranging from about 82−86°) in the dioxo complexes of these tripodal ligands. In the dioxo-bridged complexes of the tripodal ligands discussed here, smaller O−Mn−O angles correspond with longer $Mn-O_{oxo}$ bonds (see Table 5). Thus, in a dioxo-bridged complex, $\mathbf{L^3}$ may likely force a smaller O−Mn−O angle, such as it does in complex **3** and thereby also force a long and therefore weak Mn−O distance, destabilizing the dioxo-bridged com-

Table 5. Selected Bond Lengths (Å) and Angles (deg) of Dioxo-Bridged Mn^{III}_2 and $Mn^{III}Mn^{IV}$ Complexes of Tripodal Ligands[a]

	L^{1c}−$Mn^{III}Mn^{IV}$ [b]	L^{1a}−Mn^{III}_2[c]		L^{1}−Mn^{III}_2[d]
Mn−Mn (Å)	2.643(1)	2.674(4)		2.7042(5)
Mn−Ooxo (Å)	1.776(8) (Mn(IV)−O)	1.818(9)		1.8264(12)
	1.837(3) (Mn(III)−O)	1.841(1)		1.8285(12)
$Mn-N_{amine,eq}$ (Å)		2.117(8)		2.1253(14)
$Mn-N_{py,eq}$ (Å)		2.079(12)		2.1592(15)
$Mn-N_{py,ax}$ (Å)		2.353(8)		2.4044(17)
		2.386(8)		2.3982(16)
Mn−O−Mn (deg)		93.9(3)		95.44(6)
				95.80(6)
$N_{mepy}-Mn-N_{amine(eq)}$ (deg)	79.2(2)	74.2(3) ax, 74.8(3) ax		74.21(6) ax, 74.57(6) ax
		81.0(4) eq		82.26(6) eq
$N_{py}-Mn-N_{py,trans}$ (deg)		147.3(3)		147.58(6)
O−Mn−O (deg)		86.1(3)		84.56(6)
$N_{amine}-Mn-O_{tr}$ (deg)		179.1(3)		173.69(5)
$N_{py}-Mn-O_{tr}$ (deg)		174.8(3)		171.43(5)
	L^{2b}−$Mn^{III}Mn^{IV}$ [e]	L^{2a}−Mn^{IV}_2[e,f]	L^{2}−Mn^{III}_2[d]	L^{3a}−$Mn^{III}Mn^{IV}$ [g]
Mn−Mn (Å)	2.693(3)	2.747(18)	2.7067(11)	2.7393(13)
	2.691(3)		2.7119(12)	2.7379(13)
$Mn-O_{oxo}$ (Å)	1.806(4), 1.818(4)	1.750(31),	1.822(3)	1.813(3)
		1.797(28)	1.826(3)	1.811(3)
	1.823(4), 1.807(4)		1.830(2)	1.821(3)
			1.829(2)	1.819(3)
$Mn-N_{amine}$ (Å)			2.137(3)	2.114(5)
			2.149(3)	
$Mn-N_{py,eq}$ (Å)	2.081(5)		2.143(3)	2.123(4)
			2.149(3)	
$Mn-N_{py,ax}$ (Å)	2.111(5)		2.330(4)	2.134(4)
	2.118(5)		2.390(4)	2.154(5)
Mn−O−Mn (deg)	96.0(1)	101.5(15)	95.67	97.85(13)
	95.7(1)		95.80	97.92(14)
$N_{mepy}-Mn-N_{amine(eq)}$ (deg)	78.5(2) ax		73.90(13) ax	79.2(2)
	80.3(2) ax		75.63(13) ax	
$N_{ethpy}-Mn-N_{amine(eq)}$ (deg)	91.1(2) eq		93.43(13)	94.78(17) eq
				87.9(2) ax
$N_{mepy}-Mn-N_{ethpy}$ (deg)	88.1(2) ax		82.77(13)	164.36(15) tr (ax, ax)
	86.3(2) ax		90.96(13)	86.68(15) (cis ax, eq)
$N_{py}-Mn-N_{py,trans}$	158.0(2) ax		148.43(12) ax	164.36(15)
O−Mn−O (deg)	84.0(1), 84.3(1)		84.33(12)	82.15(13)
			84.20(12)	82.08(14)

[a] See Figure 1 for the structures of the ligands. [b] Towle, D. K.; Botsford, C. A.; Hodgson, D. J. *Inorg. Chim. Acta* **1988**, *141*, 167−168. [c] Goodson, P. A.; Oki, A. R.; Glerup, J.; Hodgson, D. J. *J. Am. Chem. Soc.* **1990**, *112*, 6248−54. [d] This work. [e] Oki, A.; Glerup, J.; Hodgson, D. J. *Inorg. Chem.* **1990**, *29*, 2435−2441. [f] The $Mn^{III}Mn^{IV}$ complex of thie ligand has been isolated, but the crystal structure has not been reported. [g] Schindler, S.; Water, O.; Pedersen, J. Z.; Toflund, H. *Inorg. Chim. Acta* **2000**, *303*, 215−219.

plex. Thus, the coordination of this ligand combines both the effect of larger angle equatorial chelate rings (which reduces $N_{CH_3CN}-Mn-O_{OH_2}$ and possibly the O−Mn−O angle in a dioxo-bridged complex) and methyl-substituted pyridyl donors at the axial positions, which also force the lengthening and weakening of the $Mn-O_{oxo}$ bonds and thereby contribute to destabilize the dioxo-bridged complex. These combined effects may well be factors against the formation of the dioxo complex of this ligand.

Electronic Spectra of 1 and 2. The visible region absorption spectra of complexes **1** and **2** in acetonitrile solution are similar in general features, with small shifts in absorption λ_{max} and molar absorptivities (Figure 7). Complex **1** shows peaks at 470 nm ($\epsilon = 260\ M^{-1}\ cm^{-1}$) and 495 nm (shoulder 229 $M^{-1}\ cm^{-1}$) and a weak peak at 575 nm ($\epsilon = 78\ M^{-1}\ cm^{-1}$). Complex **2** also shows absorption maxima at 440 nm (shoulder, $\epsilon = 202\ M^{-1}\ cm^{-1}$), 496 ($\epsilon = 137\ M^{-1}\ cm^{-1}$), and 570 nm ($\epsilon = 76\ M^{-1}\ cm^{-1}$). The absorption spectra of other dioxo-bridged[2b] and $Mn^{III}(\mu\text{-O})(\mu\text{-OAc})_2$[23] complexes are similar generally with two or three identifiable absorption peaks in the 400−600 nm in the visible region.[24]

Magnetic Susceptibility. The room-temperature effective magnetic moment values measured using powdered crystalline samples and calculated after correction for ligand diamagnetic contributions are 3.19 and 2.62 μ_B/dinuclear unit respectively for complexes **1** and **2**, which are within the range reported for several analogous dioxo-bridged Mn^{III}_2 complexes,[25] and 6.12 μ_B for complex **3**, which is also consistent with the literature values obtained for high-spin d^5 Mn(II) complexes.[26] The sizable difference in the magnetic moments of complexes **1** and **2**, despite the closely similar angles and distances of the dioxo bridging,[27] could be due to these small differences in the coordination angles and

(23) (a) Gultneh, Y.; Ahvazi, B.; Khan, A. R.; Butcher, R. J.; Tuchague, J. P. *Inorg. Chem*. **1995**, *34*, 2633−3645. (b) Sheats, J. E.; Czernuczewicz, R. S.; Dismukes, G. C.; Rheingold, A. L.; Petroulieas, V.; Stubbe, J.; Armstrong, W. H.; Beer, R. H.; Lippard, S. J. *J. Am. Chem. Soc*. **1987**, *109*, 1435−1444.

(24) Horner, O.; Charlot, M.-F.; Boussac, A.; Anxolabéhère-Mallart, E.; Tchertanov, L.; Guilhem, J.; Girerd, J.-J. *Eur. J. Inorg. Chem*. **1998**, 721−727.

(25) (a) Glerup, J.; Goodson, P. A.; Hazell, A.; Hazell, R.; Hodgson, D. J.; Mckenzie, C. J.; Michelsen, K.; Rychlewska, U.; Toflund, H. *Inorg. Chem*. **1994**, *33*, 4105−4111. (b) Goodson, P. A.; Oki, A. R.; Glerup, J.; Hodgson, D. J. *J. Am. Chem. Soc*. **1990**, *112*, 6248−54.

(26) (a) Gultneh, Y.; Farooq, A.; Karlin, K. D.; Liu, S.; Zubieta, J. *Inorg. Chim. Acta* **1993**, *211*, 171−175. (b) Lah, M. S.; Chun, H. *Inorg. Chem*. **1997**, *36*, 1982−1985. (c) Xiang, D. F.; Duan, C. Y.; Tan, X. S.; Hang, Q. W.; Tang, W. X. *J. Chem. Soc., Dalton Trans*. **1998**, 1201−1204.

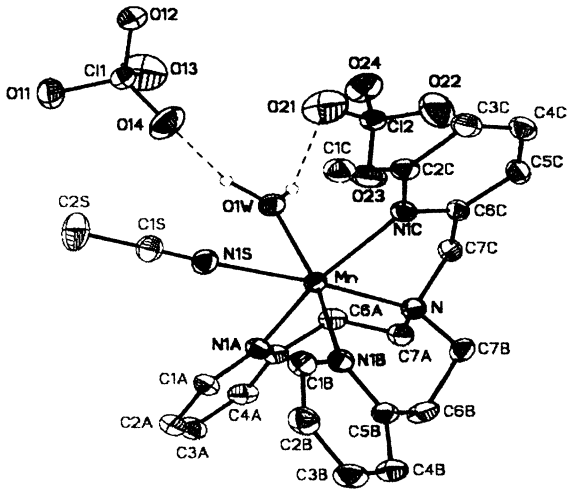

Figure 5. ORTEP drawing of the coordination in the cation of complex **3**.

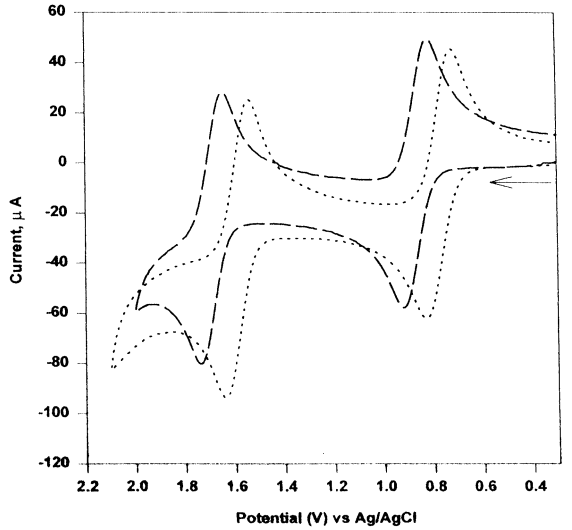

Figure 6. Cyclic Voltammograms (superimposed) of 2.0 mM solutions of complexes **1** (dashed line) and **2** (dotted line) in acetonitrile solution that is 0.1 M in *n*-Bu_4NClO_4 supporting electrolyte, using glassy carbon working, Pt counter, and Ag/AgCl reference electrodes with scan rate = 100 mV/s. The two reversible redox processes are assigned as $Mn^{III}{}_2 \leftrightarrow Mn^{III}Mn^{IV}$ ($E_{1/2}$ = 0.87 V (complex **1**), 0.78 V (complex **2**)), and $Mn^{III}Mn^{IV} \leftrightarrow Mn^{IV}{}_2$ ($E_{1/2}$ = 1.70 V (complex **1**), 1.58 V (complex **2**)) (ΔE_p = 110 mV in each case).

distances of the two different ligands. These differences have been discussed above.

Cyclic Voltammetry. The cyclic voltammograms of complexes **1** and **2** in acetonitrile solution are shown in Figure 6. Complex **1** shows two waves with peaks (vs Ag/AgCl) at $E_{1/2}$ = 0.87 V for the $Mn^{III}{}_2 \leftrightarrow Mn^{III}Mn^{IV}$ and at $E_{1/2}$ = 1.70 V for the $Mn^{III}Mn^{IV} \leftrightarrow Mn^{IV}{}_2$ reversible redox processes (ΔE_{peak} = 110 mV for each process). Complex **2** also shows two waves for the same reversible redox processes with peaks at $E_{1/2}$ (vs Ag/AgCl) = 0.78 V and at 1.58 V (average ΔE_{peak} = 110 mV). These peak potentials are the highest observed for these redox processes compared with those reported in the literature for analogous manganese complexes of this class of ligands (see below). The potentials

(27) The need for an explanation for this difference has been pointed out to us by a reviewer.

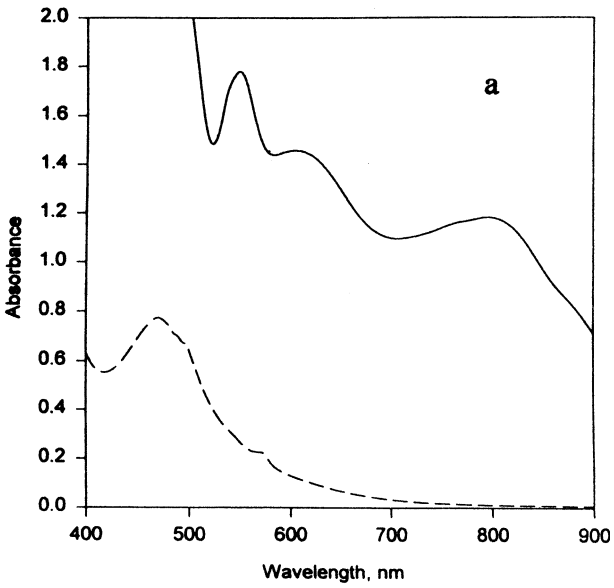

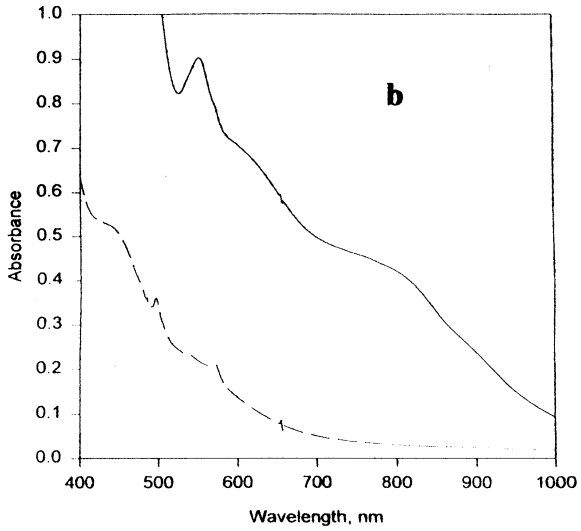

Figure 7. Visible absorption spectra of 1.0 mM solutions of complex **1** (a) and complex **2** (b) before (dashed lines) and after (solid lines) exhaustive bulk electrolytic oxidation, in acetonitrile solution, at a platinum mesh working, platinum counter, and Ag/AgCl reference electrodes, at a controlled potential of 1.98 V vs Ag/AgCl.

for the $Mn^{III}{}_2 \leftrightarrow Mn^{III}Mn^{IV}$ and $Mn^{III}Mn^{IV} \leftrightarrow Mn^{IV}{}_2$ processes are shown in Table 6 for some dioxo-bridged dinuclear manganese complexes of the tripodal ligands (2-pyridylmethyl)$_n$(2-(2-pyridyl)ethyl)$_{3-n}$)amine (n = 1−3) and their derivatives with 6-methyl substitution on the pyridyl ring of the 2-pyridylmethyl arms. These values are from this work and from the literature.

Among the series of complexes of tpa and its stepwise 6-methyl-substituted pyridyl ring derivates, there is a clear steady increase in the redox potentials with increasing number of 6-methyl substitutions, reaching a maximum at the above potentials of complexes **1** and **2**. The potentials of **1** are 0.19 and 0.29 V higher for the $Mn^{III}{}_2 \leftrightarrow Mn^{III}Mn^{IV}$ and the $Mn^{III}Mn^{IV} \leftrightarrow Mn^{IV}{}_2$ processes, respectively, than the potentials reported for these redox processes for the analogous complex of $\mathbf{L^{1a}}$ (bis(6-methyl-2-pyridylmethyl)(2-pyridylmethyl)amine), complex **1a**. The total increase in the redox potentials due to methyl substitutions at the 6-positions

Table 6. Cyclic Voltammetric Potentials (vs Ag/AgCl) of Dioxo-Bridged Dinuclear Manganese Complexes of Pyridyl Donor Tripodal Amines $[(\mathbf{L}Mn(\mu\text{-}O)_2]^{n+}$ (n = 2, 3, or 4)

	$E_{1/2}$ (V)	
L	$Mn^{III}_2 \leftrightarrow Mn^{III}Mn^{IV}$	$Mn^{III}Mn^{IV} \leftrightarrow Mn^{IV}_2$
TPA[a]	0.288	1.086
$\mathbf{L^{1b}}$ [b]	0.344	1.235
$\mathbf{L^{1a}}$ [c]	0.678	1.446
$\mathbf{L^{1}}$ [d]	0.87	1.70
$\mathbf{L^{2b}}$ [c]	0.219	1.038
$\mathbf{L^{3a}}$ [e]	0.293	1.24
$\mathbf{L^{2a}}$ [b]	0.444	1.27
$\mathbf{L^{2}}$ [d]	0.78	1.58

[a] Towle, D.; Botsford, C.; Hodgson, D. *Inorg. Chim. Acta* **1988**, *141*, 167. [b] Oki, A. R.; Glerup, J.; Hodgson, D. J. *Inorg. Chem.* **1990**, *29*, 2435−2441. [c] Goodson, P. A.; Oki, A. R.; Glerup, J.; Hodgson, D. J. *J. Am. Chem. Soc.* **1990**, *112*, 6248−6254. [d] This work. [e] Schindler, S.; Walter, O.; Pederson, J. Z.; Toflund, H. *Inorg. Chim. Acta* **2000**, *303*, 215−219.

of the three 2-pyridylmethyl donor groups in tpa (i.e. the difference in the potentials of the complexes of tpa and that of $\mathbf{L^{1}}$) is about 0.6 V for each redox process and on the average about 0.20 V/methyl substitution. The substitution of one methyl group and expansion of one chelate ring ($\mathbf{L^{2a}}$) increases these potentials by 0.16 and 0.20 V, respectively, over the potentials of the tpa complex. By contrast, there is a negligible increase in the potential of the complex of $\mathbf{L^{2b}}$ over that of tpa for one chelate ring expansion. The effect of ring expansion seems to be more pronounced in the $Mn^{III}_2 \leftrightarrow Mn^{III}Mn^{IV}$ process as indicated by comparing the difference in these potentials of complexes **2** vs **1a**, which is about 0.1 V. These observations seem to indicate the greater effect of ligand chelate ring expansions on the redox potentials of the manganese complexes when combined with ring substitutions.

Characterization of the Products of the Bulk Electrolytic Oxidation of Complexes 1 and 2. We have oxidized the Mn(III) complexes **1** and **2** by controlled-potential electrolysis at a platinum electrode. In each case, as the electrolytic oxidation commenced, the color of the solution gradually changed from brown to green over a period of about 5 min. The electrolysis was continued until the current ratio was reduced to 10% of the initial current. Coulometic measurements showed that the ratio of the total charges passed (Faradays) to the number of moles of the complex used was 1.9:1 for complex **1**and 1.8:1 for complex **2**. This amounts to close to 2-electron oxidation of each dinuclear molecule of complex, consistent with the oxidation of complexes **1** and **2** to the Mn^{IV}_2 states. Measurement of the molar conductance in acetonitrile solution of the green isolated complex after the anodic oxidation of complex **2** showed values higher and outside the range quoted for 3:1 electrolytes[28] and supports the formation of the Mn^{IV}_2 complex.

Electrolytic oxidation causes a drastic increase in the absorptions in the 400−600 nm region, from the weak absorptions of the starting Mn(III) complexes **1** and **2** (see above) to the more intense absorptions of the Mn^{IV}_2 oxidation products of complex **1** (548 nm (ϵ = 620 M^{-1} cm^{-1}), 604 nm (ϵ = 490 M^{-1} cm^{-1}), and 796 nm (ϵ = 410 M^{-1} cm^{-1})) and complex **2** (552 nm (ϵ = 310 M^{-1} cm^{-1}), 610 nm (broad shoulder, ϵ = 240 M^{-1} cm^{-1}), and 800 nm (broad shoulder, ϵ = 180 M^{-1} cm^{-1})) (Figure 7). The general features of the spectra observed here, including the wavelengths, are close to those reported for the Mn^{IV}_2 complex of tpa which has been prepared by the electrochemical oxidation of the Mn^{III}-Mn^{IV} complex.[29] The appearance of an intense absorption in the 400−500 nm region has been reported as resulting from the electrolytic oxidation of the dioxo-bridged Mn^{III}-Mn^{IV} to Mn^{IV}_2 complexes of other similar pyridyl donor ligands where the $Mn^{III}Mn^{IV}$ precursors show significantly weaker absorptions.[29−32]

We have also isolated the green Mn^{IV}_2 complex electrolytically generated from complex **2** as a powdery solid, by precipitating it from the acetonitrile solution by addition of dry ether. The absorption spectrum of this green solid, redissolved in acetonitrile, is identical to the spectrum of the original solution obtained from the Mn(II) complex/H_2O_2 reaction. Addition of aqueous H_2O_2 to the acetonitrile solution of the green complex leads to the formation of the brown Mn^{IV}_2 complex with absorption spectrum identical to that of the solution of the complex precipitated from the Mn(II) complex/H_2O_2 reaction in methanol. The addition of aqueous H_2O_2 to the Mn(II) complex of $\mathbf{L^{2}}$ first produces the green Mn^{IV}_2 complex as shown by the initial growth, with time, of the peak at 552 nm (due to Mn^{IV}_2) and subsequent diminishing overtime with simultaneous appearance and increase in intensity of the peaks at 496 and 571 nm due to the formation of the Mn^{III}_2 complex (Figure 2). The same phenomenon is exhibited by the complex **1** system.

To test whether the green complex Mn^{IV}_2, once it is formed, is reduced by the excess aqueous H_2O_2, we isolated the green precursor of complex **2** from the H_2O_2 oxidation of the Mn(II) complex of $\mathbf{L^{2}}$ and studied the kinetics of the reduction reaction spectrophotometrically under pseudo-first-order conditions. From the changes in the absorbance at 552 nm with time, the dependence of the rate on the concentrations of the complex and H_2O_2 in acetonitrile solutions were determined. First-order plots of $\log(A_0-A_t)/(A_t-A_\infty)$ vs t showed straight lines (with second-order rate constant calculated to be 0.045 M^{-1} s^{-1}) indicating that the conversion of the green Mn^{IV}_2 complex to the Mn^{III}_2 complex **2** takes place by its reduction by H_2O_2. Thus the overall reaction is the oxidation of the Mn(II) complex by H_2O_2 to the Mn^{IV}_2 green intermediate complex followed by the reduction of the Mn^{IV}_2 complexes to the stable brown Mn^{III}_2 complex **2** by excess H_2O_2. The isolated green Mn^{IV}_2 precursor of complex **2** is also reduced to the brown Mn^{III}_2 complex **2** in the presence of moisture in a reaction far slower than that with H_2O_2. The two-electron electrolytic oxidation of a dioxo-

(28) Geary, W. J. *Coord. Chem. Rev.* **1971**, *7*, 81−122.

(29) Suzuki, M.; Tokura, S.; Suhara, M.; Uehara, A. *Chem Lett.* **1988**, 477−480.

(30) Horner, O.; Charlot, M.-F.; Boussac, A.; Anxolabéherè-Mallart, E.; Tchertanov, L.; Guilhem, J.; Girerd, J.-J. *Eur. J. Inorg. Chem.* **1998**, 721−727.

(31) Goodson, P. A.; Glerup, J.; Hodgson, D. J.; Michelsen, K.; Weihe, H. *Inorg. Chem.* **1991**, *30*, 4904−4914.

(32) Goodson, P. A.; Glerup, J.; Hodgson, D. J.; Michelsen, K.; Pedersen, E. *Inorg. Chem.* **1990**, *29*, 503−508.

bridged Mn^{III}_2 complex has also been invoked in the redox cycle in the mechanism of the electrocatalytic oxidation of benzyl alcohol by such complexes.[10]

The intense absorptions in the Mn^{IV}_2 complexes have been assigned to ligand (oxo- and pyridine π-) to Mn(IV) LMCT transitions.[29] The absorptions in the region 400−700 nm that are observed in $Mn^{III}Mn^{IV}$ complexes and even more prominently in the Mn^{IV}_2 complexes are far weaker in the spectra of complexes **1** and **2** and consistent with reports on other analogous Mn^{III}_2 complexes.[33] The weak absorptions in **1** and **2** have been assigned to d−d transitions in Mn(III).

Conclusion. We have synthesized and studied the structure and cyclic voltammetric, and spectral properties of dioxo-bridged dinuclear Mn^{III}_2 complexes of a set of related tripodal pyridyl donor amine ligands with variations in steric ring substitutions and chelate ring sizes. The complexes [$\mathbf{L^1}$Mn-(μ-O)$_2$Mn$\mathbf{L^1}$](ClO$_4$)$_2$, where **L** = tris(6-methyl-2-pyridylmethyl (**1**) and L = bis(6-methyl-2-pyridylmethy)(2-(2-pyridyl)-ethyl)amine (**2**), show the highest redox potentials so far reported for manganese complexes of this class of ligands. The increase in potential is attributed to the steric effects of methyl substitutions on the pyridyl groups of the ligands and also on chelate ring expansion both of which stabilize the Mn^{III}_2 state relative to the $Mn^{III}Mn^{IV}$ and Mn^{IV}_2 states. We have shown that the bulk electrolytic oxidation of the Mn^{III}_2 complexes **1** and **2** at a controlled potential (1.98 V vs Ag/AgCl) produces the respective Mn^{IV}_2 complexes which are in turn reduced back to the Mn^{III}_2 complexes by reaction with aqueous H_2O_2. The presence of a methyl group substituent on one of the three pyridyl donor rings ortho to the N in the ligand $\mathbf{L^3}$ makes the difference in the failure of the formation of the dioxo-bridged complex by reaction of the Mn(II) complex of this ligand with aqueous H_2O_2. The green Mn^{IV}_2 complexes first formed by the reaction of the Mn(II) complexes with H_2O_2 are reduced to the Mn^{III}_2 complexes **1** and **2** by excess aqueous H_2O_2, while **1** and **2** could be electrolytically oxidized to the green Mn^{IV}_2 complexes in acetonitrile solution.

Acknowledgment. Y.G. acknowledges the support of the U.S. EPA, through the GEM program, for the support of a graduate student and the Howard University Academic Vice President's Office for Research for the funding of research laboratory supplies. R.J.B. acknowledges the DoD-ONR for funds to upgrade the diffractometer.

Supporting Information Available: Crystallographic data for complexes **1**−**3**. This material is available free of charge via the Internet at http://pubs.acs.org.

IC020131W

(33) Goodson, P.; Hodgson, D. J. *Inorg. Chem.* **1989**, *28*, 3606−2608.